Europhys. Lett., **41** (1), pp. 31-36 (1998)

Midgap states of a two-dimensional antiferromagnetic Mott-insulator: Electronic structure of meron vortices

S. John, M. Berciu and A. Golubentsev

Department of Physics, University of Toronto
60 St. George Street, Toronto, Ontario, Canada, M5S 1A7

(received 25 July 1997; accepted in final form 13 November 1997)

PACS. 71.10Fd – Lattice fermion models (Hubbard model, etc.).
PACS. 71.10Pm – Fermions in reduced dimensions (anyons, composite fermions, Luttinger liquid, etc.).
PACS. 75.50Ee – Antiferromagnetics.

Abstract. – We demonstrate from first principles that ferromagnetic core, meron vortex configurations of the spin-$\frac{1}{2}$ antiferromagnet in two-dimensions give rise to midgap electronic states in the Mott-Hubbard charge gap. Merons are collective mode excitations of the antiferromagnet and are induced by doping the system with charge carriers. They are the topological analogs of charged bosonic domain wall solitons in one-dimension.

Doped Mott insulators [1] consisting of spin-$\frac{1}{2}$ local moments exhibit a host of unconventional electronic, magnetic and optical properties [2]. These include non-Fermi- liquid transport behaviour of the metallic state, quantum spin-liquid correlations in the local moment background, and anomalous optical absorption in the mid-infrared. It has been suggested [3] that these are *intrinsic* properties of an antiferromagnetic Mott-Hubbard gap in the presence of charge carriers and that they play a central role in the occurrence of high-temperature superconductivity. While some phenomenological pictures [4], [5] of this anomalous metal have been introduced, a microscopic theory has yet to be formulated.

In this paper, we compute the electronic spectrum of antiferromagnetic (AFM) core—and ferromagnetic (FM) core—meron vortices of the spin-$\frac{1}{2}$ antiferromagnet on a bipartite, square lattice using a simple continuum approximation. These are collective mode excitations which dominate the low-energy charge excitation spectrum of the doped Mott insulator, giving rise to non–Fermi-liquid behaviour. We demonstrate that the FM-core meron induces a degenerate pair of localized electronic midgap states within the Mott-Hubbard charge gap, which are independent of the meron core radius. Electronic excitations between the Mott-Hubbard bands and these midgap levels may contribute to sub-gap optical absorption [6], [7]. Lattice effects, meron-meron interactions and meron-spin-wave interactions lead to a broadening of the midgap levels into a mid-infrared band. Translational motion of charged merons may give rise to non-Drude behaviour in the *a.c.* conductivity. Merons are the two-dimensional analogues of magnetic domain wall solitons [8], [9] in the one-dimensional antiferromagnet and they exhibit electronic properties analogous to domain walls in polyacetylene [10]. When the meron is doped with a charge carrier, its structure relaxes to that of a planar antiferromagnetic vortex with vanishing local moment amplitude in the core. We have shown that this charged meron is a bosonic collective excitation in which the localized charge resides on the induced midgap level.

Our model applies to quasi–two-dimensional systems such as the weakly coupled, layered, high-T_c oxide superconductors where finite-temperature, antiferromagnetic long-range order (LRO) is observed. It is not intended to describe a *strictly* two-dimensional system. Our picture is that of an ordered antiferromagnet at zero or low doping, in which a single added hole forms a conventional spin-polaron [11]. However, with increased doping, our numerical, Hartree-Fock calculations [12] demonstrate that these spin-polarons are unstable to the formation of charged meron-antimeron vortex pairs. We postulate that with further doping, these bound vortex pairs may dissociate giving rise to a quantum spin liquid of solitons, in which magnetic LRO is destroyed.

In our picture, spin fluctuation effects are described by the motion of these solitons and their scattering from spin waves. The time scale of electronic excitations across the Mott-Hubbard charge gap is very small compared to the time scale of magnetic fluctuations so that a well-defined, instantaneous, Mott-Hubbard gap structure exists even within the spin-liquid phase.

Consider a strongly interacting quasi–two-dimensional electron gas described by the tight-binding Hamiltonian

$$\mathcal{H} = -\sum_{\substack{\langle ij \rangle \\ \sigma}} t_{ij} (c^\dagger_{i\sigma} c_{j\sigma} + \text{h.c.}) + \sum_{ij} V_{ij} n_i n_j \,, \tag{1}$$

where $c^\dagger_{i\sigma}$ creates an electron at site i with spin σ, t_{ij} is the hopping amplitude from site j to site i on the square lattice, $n_i \equiv \sum_{\sigma=1}^{2} c^\dagger_{i\sigma} c_{i\sigma}$, and V_{ij} is the Coulomb interaction. For nearest-neighbour hopping ($t_{ij} = t_0$) and purely on-site Coulomb repulsion ($V_{ii} \equiv U$), this reduces to the Hubbard model. In order to capture the effects of spin rotation during the process of electron hopping, we retain the *nearest neighbour* Coulomb repulsion ($V_{ij} = V$). It is convenient to define the bilinear combination of electron operators $\Lambda^\mu_{ij} \equiv c^\dagger_{i\alpha} \sigma^\mu_{\alpha\beta} c_{j\beta}$, $\mu = 0, 1, 2, 3$. Here σ^0 is the 2×2 identity matrix and $\boldsymbol{\sigma} \equiv (\sigma^1, \sigma^2, \sigma^3)$ are the usual Pauli spin matrices. The quantum expectation value $\langle\ \rangle$ of this operator in mean-field theory signifies the presence of charge- and spin-density ($i = j$) and charge- and spin-current ($i \neq j$). In some previous papers, we defined the spin-flux phase [13] of the 2-d Hubbard model, and we demonstrated [14] that it has a lower Hartree-Fock ground state energy than non-flux, spiral, magnetic states (in which only the diagonal, $i = j$, components of Λ^μ_{ij} exhibit a nonzero ground state expectation value). In the spin-flux model [13], [14], we adopt the ansatz that there is no charge current in the ground state $\langle \Lambda^0_{ij} \rangle = 0$ but circulating spin-currents exist and take the form $\langle \Lambda^a_{ij} \rangle = \frac{2t_0}{V} i \Delta_{ij} \hat{n}_a$, $a = 1, 2, 3$, where $|\Delta_{ij}| = \Delta$ for all i and j, and $\hat{n}$ is a unit vector. We conjecture that spin-flux is a hidden "law of nature" which is hidden in models which neglect the non-zero range of the Coulomb interaction.

Using the Pauli matrix identity, $\frac{1}{2} \sigma^\mu_{\alpha\beta} (\sigma^\mu_{\alpha'\beta'})^* = \delta_{\alpha\alpha'} \delta_{\beta\beta'}$, it is possible to rewrite the electron-electron interaction term as follows: $n_i n_j = (2 + \delta_{ij}) n_i - \frac{1}{2} \Lambda^\mu_{ij} (\Lambda^\mu_{ij})^\dagger$. Using the Hartree-Fock factorization, $\Lambda^\mu_{ij} (\Lambda^\mu_{ij})^\dagger \to \langle \Lambda^\mu_{ij} \rangle (\Lambda^\mu_{ij})^\dagger + \Lambda^\mu_{ij} \langle \Lambda^\mu_{ij} \rangle^* - \langle \Lambda^\mu_{ij} \rangle \langle \Lambda^\mu_{ij} \rangle^*$, we obtain the mean-field Hamiltonian

$$\mathcal{H}^{\text{MF}} = -t \sum_{\langle ij \rangle} c^\dagger_{i\alpha} T^{ij}_{\alpha\beta} c_{j\beta} + \text{h.c.} + U \sum_{i} c^\dagger_{i\alpha} (\mathbf{s}_i \cdot \boldsymbol{\sigma}_{\alpha\beta}) c_{i\beta} \,. \tag{2}$$

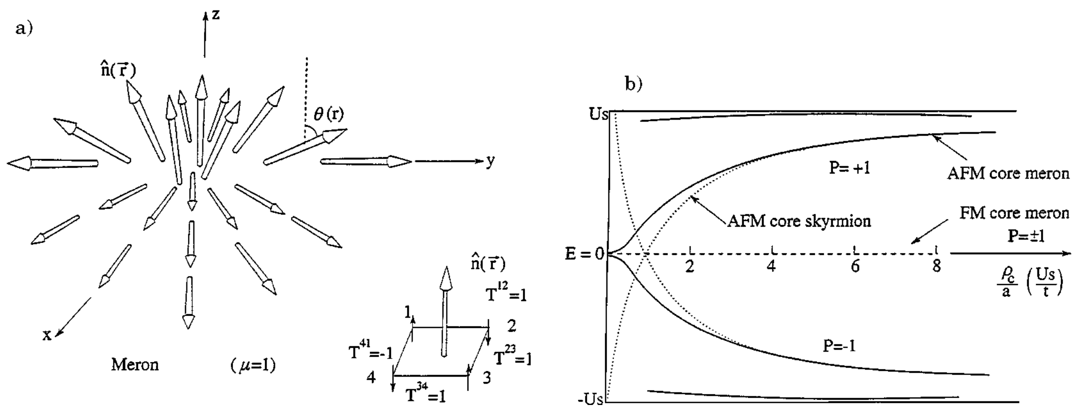

Fig. 1. – a) The 2-d analog of the domain wall is a meron texture depicted as a lotus flower configuration of the local director field $\hat{n}(\mathbf{r})$. We associate a unit cell of four sites with local moments aligned antiferromagnetically with each $\hat{n}(\mathbf{r})$. Each plaquette exhibits a spin-flux of π ($T^{12}T^{23}T^{34}T^{41} = -1$) corresponding to a 2π rotation of the internal coordinate system of the electron as it encircles the plaquette. This is a dynamical consequence of the nearest neighbour Coulomb repulsion. As $\hat{n}(\mathbf{r})$ varies smoothly from one unit cell to the next, it makes a half-covering of the unit sphere S_2. b) The antiferromagnetic-core meron exhibits a pair of nondegenerate, localized, subgap electronic levels in the 2-d Mott-Hubbard charge gap. These levels (solid lines) are plotted as a function of the *dimensionless* meron core radius. Both levels approach the midgap ($E = 0$) as the core radius $\rho_c \to 0$ as well as in the limit of small local moment amplitude ($Us \ll t$). Some higher angular momentum bound states also appear near the upper and lower Mott-Hubbard band-edges $\pm Us$. On the other hand, the ferromagnetic-core meron has a doubly degenerate midgap state (dashed line) which is independent of core radius. Finally, the nondegenerate $\ell = 0$ states for the fluxless skyrmion are depicted with dotted lines.

Here, $T^{ij}_{\alpha\beta} \equiv (\delta_{\alpha\beta} + i\Delta_{ij}\hat{n}\cdot\boldsymbol{\sigma}_{\alpha\beta})/\sqrt{1+\Delta^2}$ are spin-dependent $SU(2)$ hopping matrix elements defined by mean-field theory, $\mathbf{s} \equiv \frac{1}{2}\langle c^{\dagger}_{i\alpha}\boldsymbol{\sigma}_{\alpha\beta}c_{i\beta}\rangle$ is the local moment amplitude, and $t = t_0\sqrt{1+\Delta^2}$. In deriving (2) we have dropped constant terms which simply change the zero of energy in (1) as well as terms proportional to $\sum_i n_i$ which simply change the chemical potential. It was shown previously [14] that the ground-state energy depends only on the plaquette matrix product (see fig. 1 a)) $T^{12}T^{23}T^{34}T^{41} \equiv \exp[i\hat{n}\cdot\boldsymbol{\sigma}\Phi]$. Here, Φ is the spin-flux which passes through each plaquette and 2Φ is the angle through which the internal coordinate system of the electron rotates as it encircles the plaquette. This corresponds to a new broken symmetry in which the mean-field Hamiltonian acquires a term with the symmetry of a spin-orbit interaction. We now proceed to demonstrate that mid-gap states may be formed within the antiferromagnetic Mott-Hubbard charge gap within the $\Phi = \pi$ spin-flux phase for the FM-core meron configuration of $\mathbf{s}_i$.

A meron vortex in the plaquette director field $\hat{n}$ is depicted in fig. 1 a). We consider a local moment configuration $\{\mathbf{s}_i\}$ which follows the axis of the director within a given plaquette, while the director field varies smoothly from one plaquette to the next in the form of a lotus flower. As the director field rotates to an angle (θ, ϕ) from the z-direction, the spins on one sublattice rotate by the same angles (θ, ϕ), while the spins on the other sublattice rotate to $(\pi - \theta, \pi + \phi)$. We refer to this collective excitation as an AFM-core meron. On the other hand, it is interesting to consider an FM-core meron in which the local moments are ferromagnetically polarized about the plaquette vector, $\hat{n}$, at $\mathbf{r} = 0$. As the director field, $\hat{n}$, rotates to (θ, ϕ), the spins on one sublattice (say sites 1 and 3) rotate to (θ, ϕ), whereas the spins on the second sublattice (sites 2 and 4) rotate to $(\theta, \pi + \phi)$. As $r \to \infty$, $\theta \to \pi/2$, leading once again to local AFM order far from the core region. We refer to this excitation as an FM-core meron. The evaluation of the electronic structure of both merons is facilitated by considering a mean-field background of uniform spin-flux of π through each elementary plaquette of a 2-d square lattice. In the absence of second-nearest-neighbour hopping a flux of π is equivalent to a flux of $-\pi$ and there is no breaking of chiral symmetry. Defining the unit cell to consist of the four elementary sites of a plaquette (see fig. 1 a)), we introduce an eight-component electron field operator $\psi^\dagger(\mathbf{r}) \equiv [\chi^{+(1)}, \chi^{+(2)}, \chi^{+(3)}, \chi^{+(4)}]$, where $\chi^{+(j)} \equiv (c^\dagger_{j\uparrow}, c^\dagger_{j\downarrow})$ denotes up and down spin electron creation operators. The mean-field Hamiltonian (2) may then be re-expressed in terms of 8×8 matrices α_x, α_y, and β:

$$\mathcal{H}^{\mathrm{MF}} = \sum_{\mathbf{k}} \psi^\dagger_{\mathbf{k}} [\epsilon_{k_x} \alpha_x + \epsilon_{k_y} \alpha_y + (Us)\beta] \psi_{\mathbf{k}} \,. \tag{3}$$

Here, we have introduced the Fourier transform $\psi_{\mathbf{k}} \equiv N^{-1/2} \Sigma_{\mathbf{r}} e^{-i\mathbf{k}\cdot\mathbf{r}} \psi(\mathbf{r})$, where N is the number of unit cells in the square lattice, $\epsilon_k \equiv -2t \cos ka$, and a is the lattice constant. The structure of the matrices α_x, α_y and β is determined by our choice of mean-field order parameters $\langle \Lambda^\mu_{ij} \rangle$ and $\mathbf{s}_i$. We choose the product of $SU(2)$ matrices T^{ij} around each elementary square of the lattice to be *minus* one using a *spin-independent gauge* in which $T^{ij} = -1$ for one link of each plaquette, but $T^{ij} = +1$ for the remaining three links (see fig. 1 a)).

In this *spin-independent gauge* $\alpha_x = -\gamma_z \otimes \tau_x \otimes I$ and $\alpha_y = \gamma_x \otimes \tau_x \otimes I$ contain the identity matrix in spin-space and $\beta = I \otimes \tau_z \otimes (\boldsymbol{\sigma} \cdot \hat{n})$. Here, I is the 2×2 identity matrix, $\boldsymbol{\gamma}$ and $\boldsymbol{\tau}$ are two sets of 2×2 Pauli matrices describing *hopping* in the x- and y-directions respectively, and $\boldsymbol{\sigma}$ are the usual 2×2 Pauli matrices which act on the *internal* spin-space of the electron. A detailed derivation of these matrices has been given in ref. [14]. Hereafter we drop the direct product symbol $\otimes$ for convenience.

For a spatially non-varying director field $\hat{n}(\mathbf{r}) = \hat{z}$, the band edges of the effective one-electron Mott-Hubbard charge gap occur at the four corners $\mathbf{k} = \frac{\pi}{2a}(\pm 1, \pm 1)$ of the reduced Brillouin zone. Linearizing the dispersion relations in (3) about these points yields an effective continuum Schrödinger equation $H_{\mathrm{eff}} \psi = E\psi$, where

$$H_{\mathrm{eff}} = i\alpha_x \partial_x + i\alpha_y \partial_y + A\tau_z (\boldsymbol{\sigma} \cdot \hat{n}) \,, \tag{4}$$

where the dimensionless coordinate variables x and y are measured in units of $(2ta/Us)$ and the dimensionless energy E is measured in units of Us. In eq. (4) the local moments are rigidly aligned either antiferromagnetically (if $A = I$), or ferromagnetically (if $A = \tau_z$), with respect the unit vector $\hat{n}(\mathbf{r})$. As a result, vorticity in the director field does not lead to intra-plaquette phase vorticity and the resulting solitons do not carry spin-flux over and above the background. The possibility of an FM- core soliton ($A = \tau_z$) with an AFM background will be introduced in what follows by generalizing the interaction $\boldsymbol{\sigma} \cdot \hat{n}$ to have different structure for the two separate sublattices.

Consider an axially symmetric magnetic texture in which the director field $\hat{n}(\mathbf{r})$ exhibits integer μ units of vorticity: $\boldsymbol{\sigma} \cdot \hat{n}(\mathbf{r}) \to U^\dagger(\mathbf{r}) \sigma_z U(\mathbf{r})$, where $U(\mathbf{r}) = e^{i\theta(r) A \sigma_y/2} e^{i\mu\phi\sigma_z/2}$. Here (r, ϕ) are polar coordinates and $\theta(r)$ is an arbitrary function of the radial coordinate with boundary conditions $\theta(0) = 0$ and $\theta(\infty) = \pi/2$ (meron) or $\theta(\infty) = \pi$ (skyrmion). The AFM-core solitons correspond to the choice $A = I$ and the FM-core solitons correspond to the choice $A = \tau_z$. Using the substitution $\psi = e^{i(\alpha_z + \mu\sigma_z + 2\ell)\phi/2} \eta(r)/\sqrt{r}$, the *radial* Schrödinger equation becomes $H_{\mathrm{r}} \eta = E\eta$, where

$$H_{\mathrm{r}} \equiv i\alpha_x \partial_r + \frac{\alpha_y}{r} \left(\frac{\mu}{2} \sigma_z + \ell \right) + A\tau_z \sigma(r) \,. \tag{5}$$

Here, $\sigma(r) \equiv e^{-i\theta A\sigma_y/2}\sigma_z e^{i\theta A\sigma_y/2}$ and ℓ is the angular-momentum quantum number. Since the meron does not carry additional spin-flux, only integer values of ℓ are allowed. The solution of (5) is simplified by noting that the plaquette parity operator $P \equiv \tau_z\gamma_y$ commutes with $H_{\rm r}$. It follows that the eigenfunctions of $H_{\rm r}$ can be labelled according to the eigenvalues of P, which we denote as $s_1 = \pm 1$. Introducing the unitary matrix $U_1 = e^{i\frac{\pi}{4}\gamma_x\tau_z}$, and noting the $U_1^\dagger P U_1 = \gamma_z$, the transformed radial equation becomes

$$\left\{-is_1\tau_x\partial_r + \frac{\tau_y}{r}\left(\frac{\mu}{2}\sigma_z + \ell\right) + A\tau_z(\sigma_z\cos\theta + \sigma_x A\sin\theta)\right\}\eta = E\eta\,. \tag{6}$$

For either the FM-core or AFM-core solitons, if η is an eigenfunction of (6) with quantum numbers (E, s_1, ℓ), it follows that $\sigma_y\eta$ is another eigenfunction with quantum numbers $(-E, -s_1, -\ell)$. Therefore the spectrum is always symmetric about $E = 0$.

For the AFM-core soliton ($A = I$), it follows that $\tau_x\sigma_y\eta$ is another eigenfunction with quantum numbers $(E, s_1, -\ell)$. As a consequence, the $\ell \neq 0$ levels of the AFM-core solitons are doubly degenerate whereas the $\ell = 0$ levels are non-degenerate.

For the FM core soliton ($A = \tau_z$), the state $\tau_y\sigma_z\eta$ is another eigenfunction with quantum numbers $(E, -s_1, \ell)$. As a consequence, all of the levels of the FM-core soliton are doubly degenerate.

We have solved eq. (6) for the meron configuration $(\mu = 1), \theta(r) = 2\tan^{-1}(r/\rho_{\rm c})$ for $r < \rho_{\rm c}$ and $\pi/2$ for $r > \rho_{\rm c}$, as a function of the meron "core radius" $\rho_{\rm c}$. Depicted as solid lines in fig. 1 b) are the two *nondegenerate* $\ell = 0$ states of the AFM core meron. Both states approach the midgap $E = 0$ as the dimensionless parameter $(\frac{U_S}{t})\frac{\rho_{\rm c}}{a} \to 0$. All other ($\ell \neq 0$) bound states remain close to the Mott-Hubbard band edges. For the non–flux-carrying AFM-core skyrmion, $A = I$ and $\theta(r) = 2\tan^{-1}(r/\rho_{\rm c})$ for all r. In this case a non-degenerate $P = 1$ state emerges from the upper band edge for large ρ_c and eventually joins the lower band edge as $\rho_{\rm c} \to 0$. Likewise a $P = -1$ state moves from the lower band edge and merges into the upper continuum. This is depicted by dotted lines in fig. 1 b). Finally, the doubly degenerate $\ell = 0$ states of the FM-core meron are depicted as a dashed line at precisely $E = 0$ for all values of $\rho_{\rm c}$.

Unlike the neutral meron configurations which have a lotus flower structure, charged merons induced by doping exhibit a planar vortex structure. This can be described by setting $\cos\theta \equiv 0$ in eq. (6), while retaining the parameterization $\sin\theta = \tanh(r/\rho_{\rm c})$. It is straightforward to verify that eq. (6) for the doped meron has a doubly-degenerate mid-gap level, whose wave functions are given by $\eta^\dagger(r) = \sqrt{r}\,\mathrm{sech}(r/\rho_{\rm c})\,(1,0,-1,0)$ for $s_1 = 1$ and $\eta^\dagger(r) = \sqrt{r}\,\mathrm{sech}(r/\rho_{\rm c})\,(0,1,0,-1)$ for $s_1 = -1$. For hole doping, the gap states are empty and the valence band continuum states are fully occupied. It is easy to verify that these occupied states are spin-paired and that this charged vortex soliton is a bosonic collective excitation which carries no net spin. In analogy with polyacetylene, this suggests a possible microscopic origin for non-Fermi liquid behaviour in the doped copper-oxide superconductors through the mechanism of charge-spin separation of the added holes.

The importance of meron configurations to the observed non–Fermi-liquid behaviour of a doped, quasi–two-dimensional Mott-Hubbard system is determined by the free-energy of a quantum liquid of such solitons in thermodynamic equilibrium. Our study [12] suggests that when a hole is added to the undoped system, the energy of the extra charge carrier is minimized if it nucleates a magnetic (skyrmion) spin-polaron and it resides in the associated sub-gap electronic level. This is analogous to polaron formation in polyacetylene [10]. Unlike one-dimensional polyacetylene, in which the addition of a second charge carrier leads to the immediate dissociation of the polaron into a pair of charged, bosonic, domain wall solitons, the two-dimensional antiferromagnet is driven by entropic as well as energetic effects. At low doping, charge carriers remain bound in meron-antimeron configurations. It has been suggested [15] within the context of the long-wavelength, continuum, $O(3)$ nonlinear σ-model that at finite temperature, the liquid of spin-polarons may undergo a Kosterlitz-Thouless [16] type of phase transition into a (quantum) Coulomb plasma of free merons. It is important to re-examine this possibility in the presence of spin-flux and charged, bosonic merons. These topological effects are distinct from previously considered [17] spin-wave renormalization effects. A microscopic derivation [18] of the $O(3)$ σ-model from the Hubbard model, further suggests that this phase transition may be driven by increased doping even at fixed temperature. The effect of clothing the doping electrons (or holes) with merons leads to a pinning of the chemical potential near the center of the Mott-Hubbard charge gap. It leads to the emergence of an impurity band near $E = 0$ as the system is doped accompanied by a quantum liquid of merons in which long-range AFM order is absent. Behaviour of this type as well as evidence for charge-spin separation is observed in angle-resolved photo-emission experiments [19]-[21].

***

This work was supported in part by the Natural Sciences and Engineering Research Council of Canada.

REFERENCES

[1] Mott N. F., *Proc. Phys. Soc. London A*, **62** (1949)416; *Rev. Mod. Phys.*, **40** (1968) 677.
[2] See for instance *Physical Properties of High-Temperature Superconductors*, Vol. **I-III** edited by D. Ginsburg (World Scientific) 1992.
[3] Anderson P. W., *Science*, **235** (1987)1196.
[4] Varma C. M. *et al.*, *Phys. Rev. Lett.*, **64** (1990) 497.
[5] Anderson P. W., *Phys. Rev. Lett.*, **64** (1990) 1839.
[6] Uchida S. *et al.*, *Phys. Rev. B*, **43**(1991) 7942.
[7] Thomas G. A., in *Proceedings of the 39th Scottish Universities Summer School in Physics, St. Andrews* (Adam Hilger, New York) 1991.
[8] Schultz H. J., *J. Phys.* (*Paris*), **50** (1989) 2833.
[9] Poilblanc D. and Rice T. M., *Phys. Rev. B*, **39** (1989) 9749.
[10] See for instance, Heeger A. J., Kivelson S., Schrieffer J. R. and Su W. P., *Rev. Mod. Phys.*, **60** (3) (1988) 781.
[11] Schrieffer J. R. *et al.*, *Phys. Rev. Lett.*, **60** (1988) 944; Schrieffer J. R. *et al.*, *Phys. Rev. B*, **39** (1989) 11663.
[12] Berciu M. and John S., to be published in *Phys. Rev. B.*
[13] John S. and Golubentsev A., *Phys. Rev. Lett.*, **71** (1993) 3343; John S. and Golubentsev A., *Phys. Rev. B*, **51** (1995) 381.
[14] John S. and Müller-Groeling A., *Phys. Rev.*, **51** (1995) 12989.
[15] Gross D. J., *Nucl. Phys. B*, **132** (1978) 439.
[16] Kosterlitz J. and Thouless D., *J. Phys. C*, **6** (1973) 1181; Kosterlitz J., *J. Phys. C*, **7** (1974) 1046.
[17] Chakravarty S., Halperin B. I. and Nelson D. R., *Phys. Rev. Lett.*, **60** (1988) 1057
[18] John S., Voruganti P. and Goff W., *Phys. Rev. B*, **43** (1991) 10815.
[19] Anderson R. O. *et al.*, *Phys. Rev. Lett.*, **70** (1993) 3163.
[20] Laughlin R. B., *Phys. Rev. Lett.*, **79** (1997) 1726.
[21] Marshall D. S. *et al.*, *Phys. Rev. Lett.*, **76** (1996) 4841; Loeser A. G. *et al.*, *Science*, **273** (1996) 3235; Ding H. *et al.*, *Nature* (*London*), **382** (1996) 51.